

Opening a Bandgap in Graphene graphene nanoribbon and bilayer graphene

Yuan Sui

School of Physics, Peking University

Seminar for Solid State Physics, Oct 2022

Contents

1 Opening a bandgap in graphene nanoribbon

- Fundamentals
- Experiments and results

2 Opening a bandgap in bilayer graphene

- Fundamentals
- Potassium doping
- Graphene bilayer FET

Contents

1 Opening a bandgap in graphene nanoribbon

- Fundamentals
- Experiments and results

2 Opening a bandgap in bilayer graphene

- Fundamentals
- Potassium doping
- Graphene bilayer FET

GNR electronic states

- the electronic states of GNR largely depend on the edge structures (armchair or zigzag)
- zigzag GNR is always metallic while armchair is semiconducting with an energy gap scaling with the inverse of the GNR width

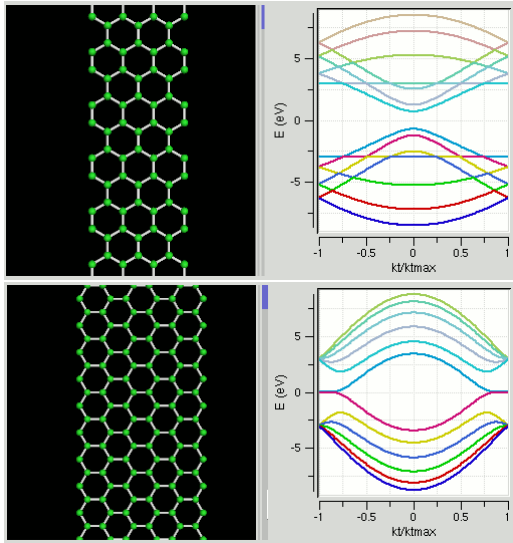


Figure 1: Band structure of armchair and zigzag graphene nanoribbon

Energy Band-Gap Engineering of Graphene Nanoribbons

PRL 98, 206805 (2007)

Devices and phenomenon

- define nanoribbons with widths by HSQ
- schottky barrier formation, heavily doped silicon substrate
- larger energy gaps in narrower GNRs

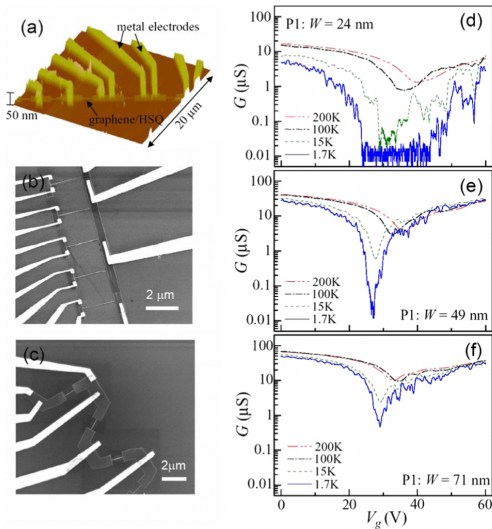


Figure 2: GNR devices and its conductance

Conductance vs width

- $V_g - V_{Dirac} = -50V$
- $G = \sigma(W - W_0)L$
- finite W_0 measured

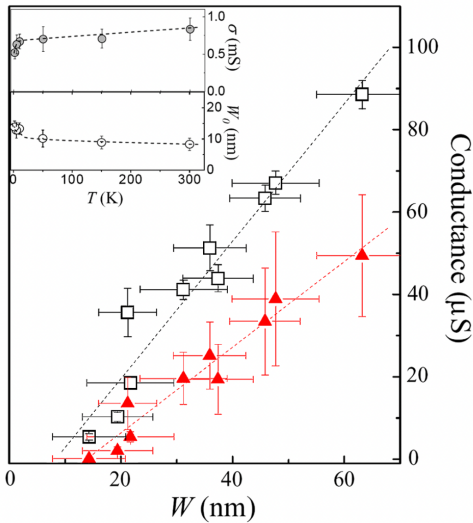


Figure 3: Conductance-width relation

Quantitative scaling

- the bandgap can be directly obtained from the value of V_b at the vertex of the diamond
- $E_{gap} = \alpha / (W - W^*)$

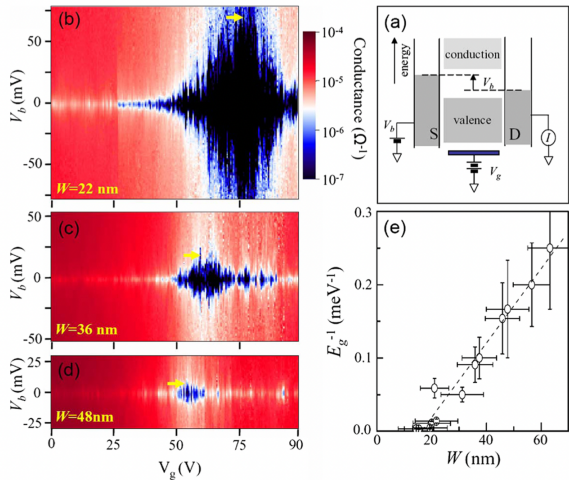


Figure 4: Quantitative scaling of bandgap

Different crystallographic directions

- overall scaling of E_{gap} as a function of W for six different device sets
- randomly scattered values around the average E_{gap} corresponding to W with no sign of crystallographic directional dependence

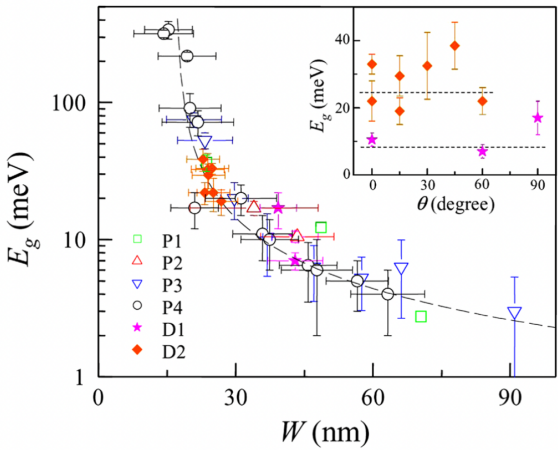


Figure 5: Similar scaling behavior in different crystallographic directions

Contents

1 Opening a bandgap in graphene nanoribbon

- Fundamentals
- Experiments and results

2 Opening a bandgap in bilayer graphene

- Fundamentals
- Potassium doping
- Graphene bilayer FET

Bilayer graphene

AA-stacked and AB-stacked

$$\varepsilon_\alpha(k) = \pm \left[\frac{\gamma_1^2}{2} + \frac{U^2}{4} + \left(v^2 + \frac{v_3^2}{2} \right) k^2 + (-1)^\alpha \sqrt{\Gamma} \right]^{1/2}$$

where the band index $\alpha = 1, 2$ and

$$\Gamma = \frac{1}{4}(\gamma_1^2 - v_3^2 k^2)^2 +$$

$$v^2 k^3 (\gamma_1^2 + U^2 + v_3^2 k^2) + 2\gamma_1 v_3 v^2 k^3 \cos 3\phi$$

and $v_3 = \sqrt{3} a \gamma_3 / 2\hbar$.

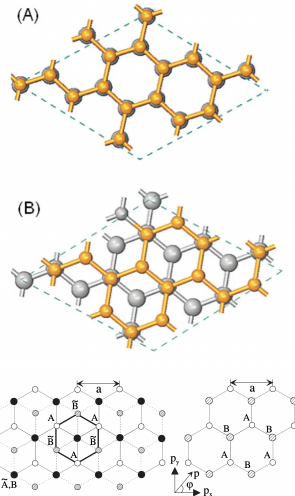


Figure 6: AA-stacked and AB-stacked bilayer graphene

Controlling the Electronic Structure of Bilayer Graphene

Science 313, 951 (2006)

Dispersion relation

- the 0.4eV splitting of the p state confirms that the sample is composed predominantly of two graphene layers
- the crossing point can be clearly observed because this bilayer is n-type-doped through carrier depletion from the SiC substrate

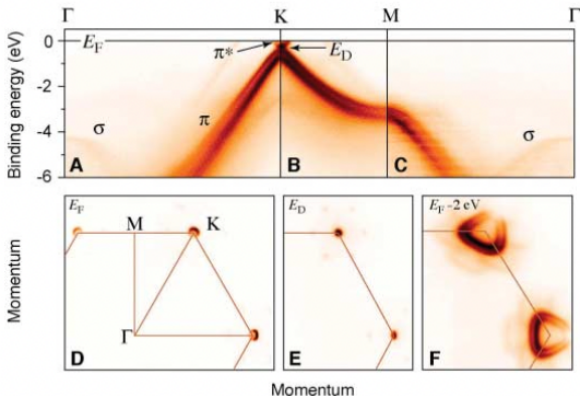


Figure 7: Dispersion relation by ARPES

Doping effects

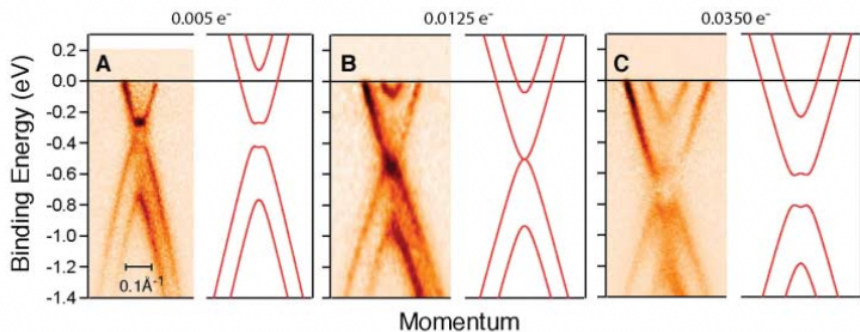


Figure 8: open-close-reopen through Potassium doping

Doping effects

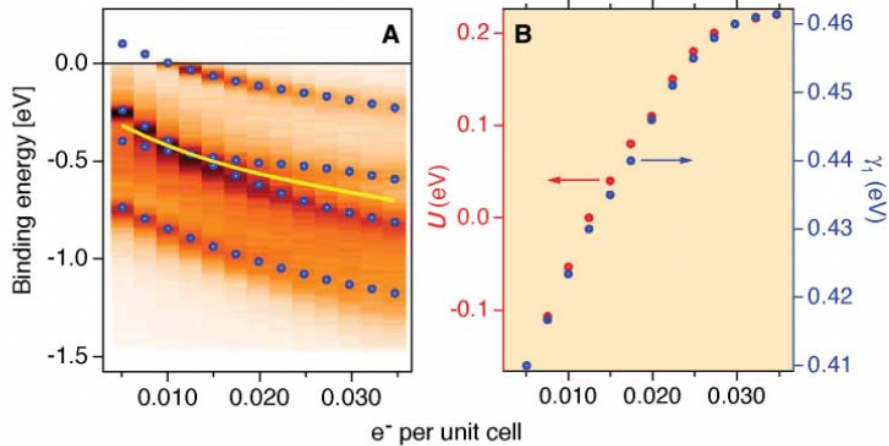


Figure 9: open-close-reopen through Potassium doping

Direct observation of a widely tunable bandgap in bilayer graphene
Nature 459, 820 (2009)

Graphene bilayer FET

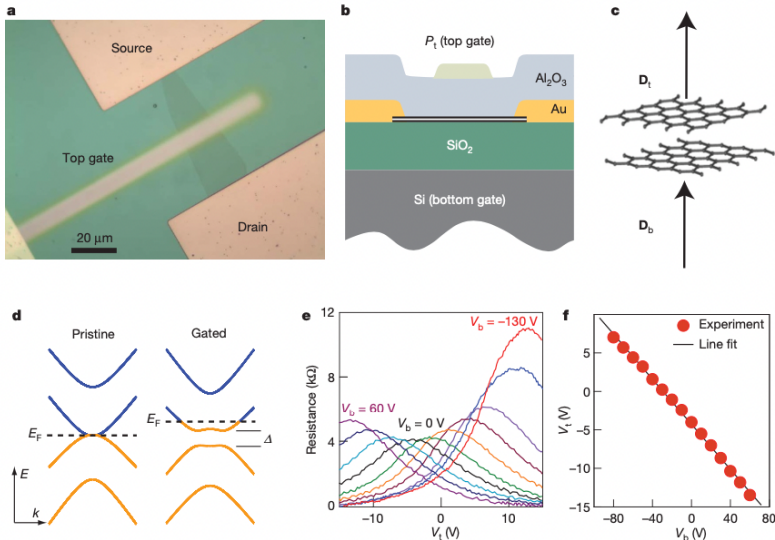


Figure 10: Graphene bilayer FET

Graphene bilayer FET

- $\delta D = D_b - D_t, \quad \bar{D} = (D_b + D_t)/2$
- $D_b = +\varepsilon_b(V_b - V_b^0)/d_b, \quad D_t = -\varepsilon_t(V_t - V_t^0)/d_t, \quad k = -\varepsilon_b d_t / \varepsilon_t d_b$
- individual control of net carrier doping and breaking the inversion symmetry of the bilayer

Infrared microspectroscopy

- a gate-dependent peak below 300 meV and a dip centred around 400 meV
- the bandgap can be continuously tuned up to at least 250 meV by electrical gating

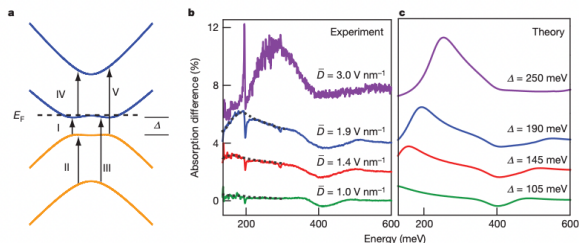


Figure 11: Infrared microspectroscopy

Infrared microspectroscopy

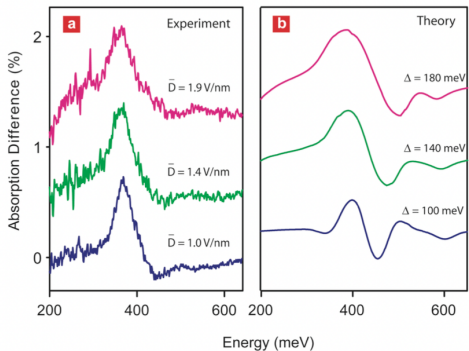
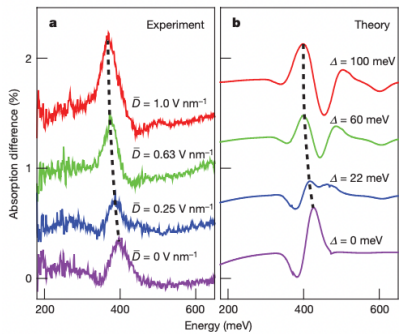


Figure 11: Infrared microspectroscopy